International Conference on Applied Energy 2020
Dec. 1 - Dec. 10, 2020, Bangkok / Virtual
Paper ID: 640

Numerical Investigations of the Junction Temperature at Different Cold Plate Design configurations with and without Thermal Interface Material

Thamer Khalif Salem[1], Mohammed Ridha Jawad Al-Tameemi [2*], Zhibin Yu[3]

1 Department of Mechanical Engineering, Tikrit University, Tikrit, Iraq.

2 College of Engineering, University of Diyala, Baqubah, Iraq. (Corresponding Author).

3 Systems, Power & Energy Research Division, School of Engineering, University of Glasgow, Glasgow G12 8QQ, UK.

ABSTRACT

Cold plates are one of the most commonly used cooling methods in compact electronics circuits. This cooling system operates through conduction and forced convection heat transfer. To identify the optimum design of a cold plate that can dissipate up to 100 W/cm^2 of heat generated from an electronic chip, three models are proposed and analyzed theoretically. Star CCM+ and EES program are used to conduct the simulation. In model 1 and 2, the cold plate material is Aluminum, while Copper is used in model 3. The use of thermal interface material (TIM) was also investigated and compare to a similar model without TIM. In addition, the effects of various design parameters on the junction temperature have been studied. The results show that using Copper as a cold plate material with a pipe diameter of 8 mm have resulted in 16.3 % reduction in junction temperature compared to model 1. The validation is performed by comparing results obtained from both software for model 1 without TIM, which showed a good agreement between them.

Keywords: TIM, Cold plate material and geometry, Numerical analysis, Junction temperature.

NONMENCLATURE

Abbreviations

EES	Engineering equation solver
MCN	Mesh cells number
TIM	Thermal interface material

Symbols

A	Surface area, (m^2)
Cp	specific heat, (kJ/kg.K)
d_p	Pipe diameter, (m)
$\bar{h}$	Average heat transfer coefficient (W/m^2.K)
k	Thermal conductivity, (W/m.K)
L	Length, (m)
$\dot{m}$	Mass flow rate, (kg/s)
n	Number of cold plate pass, (-)
r	Radius, (m)
R	Thermal resistance, (K/W)
S_p	Space between chips, (m)
t	Thickness, (m)
T	Temperature, (°C)
W	width, (m)

1. INTRODUCTION

Nowadays, the demand for high accuracy in computational analysis is increased with the rise in problems complexity associated with modern scientific computation such as 3D modeling and image processing. Such demand usually met by increasing the numbers of processors (CPU) which will consequently lead to higher electrical power consumption. As a consequence, the heat generated from these appliances will rise sharply; requiring more efficient cooling technique. In general, there are two methods to cool down the chips, the heat sink and the cold plate [1]. Numbers of scientific researches revealed that liquid cooling using cold plate is more efficient than air cooling by heat sink [2], [3]. For instant, cold plate can achieve

2-10 time better quality of performance than the conventional fan cooling [1].

Six models of cold plates with variable channels have been numerically investigated by Choi et al. [4]. The results showed that with the increment in heat flux, serpentine models achieved the highest performance with a lower pressure drop than the other models[4][4][4]. Raaid and Thamer [5] experimentally and numerically investigated the effects of various design factors on the finned cold plat performance. For Reynold number ranged from 756 to 11353, the cold plate can dissipate 53 % of the heat. Haifeng, et al. [6] have optimized a liquid cold plate to control the working temperature of electrical vehicle batteries. The results show that plate configuration can significantly influence the operating range of temperature. In addition, the performance of cold plate can be enhanced by decreasing the pressure flow lost and vortex region. Wang, et al.[7] Designed and simulated a cold plate to prevent thermal damage in a hybrid electric vehicle battery. The numerical results showed the proposed model can keep the battery temperature range within 2 to 3 °C.

Various thermal integrated material (TIM) has been used in combination with cold plates. Kalaprasad et al.[8] have used sisal, glass, and hybrid fiber reinforced polyethylene as a TIM composite material. The impact of adding carbon fiber to polypropylene on the thermal conductivity of composite plastic was investigated by Kuriger and Alam [9]. The thermal conductivity of TIM was measured in two directions longitudinal and transverse. The experimental study is tested at different volumetric percentages of carbon fiber material of 9 %, 17 %, and 23 %. The results showed that the thermal conductivity in the longitudinal direction increased with the rise in volumetric percentage of carbon fiber, while maintain constant at 2.46 $Wm^{-1}K^{-1}$ in the transverse directions. Kim et al. [10] studied the thermal conductivity of polymer and Graphene Nano (GN). The experimental results demonstrated an improvement in the thermal conductivity by 121 % at 20 wt% of GN interface. In addition, the conductivity of bulk and in-plane TIM types incremented by 650 % and 2.9% respectively compared to the polymer interface material. Carbon fiber reinforced epoxy was used as TIM in a heat sink by Thamer et al. [11]. The study is analyzed at different ratios of carbon fiber and epoxy. The results demonstrated that the performance of heat sink increases with the increment in carbon fiber percentage that added onto the epoxy.

From the literature reviews, there is limited studies that compare the performance of cold plate with and without TIM in terms of thermal resistant, coolant mass flow, pipe diameters and material and chip distance. The current study aims to numerically investigate these objectives. Thus, two cases of cold plate with and without TIM are proposed. Furthermore, three models were investigate under the above design parameters. In model 1 and 2, the cold plate material is Aluminum while model 3 is Copper. In addition, this study is designed to identify the optimum cold plate configuration that can maintain the junction temperature below 100 °C to protect electronic chips from thermal damage.

2. MATHEMATICAL MODELLING

In the present research, the numerical investigations is conducted using Star CCM+ software and EES program. The schematic diagram for model 1 and 2 is shown in Figure 1. In these models, water has been used to cool five power chips which is fabricated from silicon material with a dimension of 20×20×5 mm as illustrated in Figure 1 (A and B).

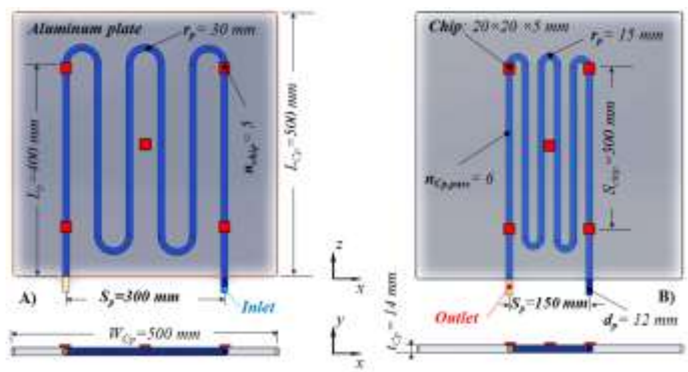

Figure 1. Schematic diagram of top and front view of the cooling plates A) model 1 and B) model 2.

The space between chips (S_p) for model 1 and 2 are set as 300 and 150 mm, respectively. The water coolant inlet temperature is set at 20 °C. The TIM specification is 0.1 mm thickness and 1 W/m·K thermal conductivity. Pipe diameters ranged from 1 to 20 mm and liquid mass flow rate from 0.05 to 0.4 kg/s. The 1D mathematical model for these two case studies is shown in Figure 2.

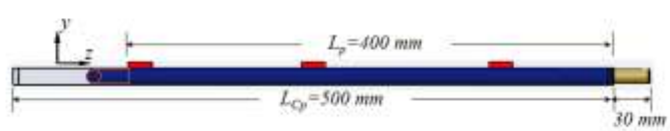

Figure 2. Right side view of one dimensional cold plate

The thermal resistance for each components of the cold plate has been determined as a function of junction temperature. The effects of design parameters on the junction temperature have been calculated based on the thermal resistance network of the system with and without TIM as shown in Figure 3 (A and B).

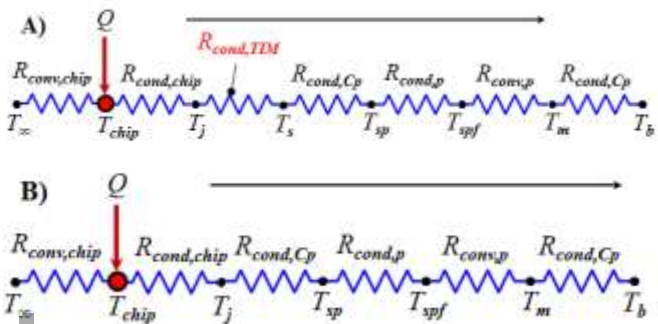

Figure 3. The thermal resistance network of the cold plate A) With TIM and B) without TIM.

It is assumed that there is no heat lost to the environment. The thermal resistances of the cold plate can be calculated using Fourier's law and Newton's cooling law equations as follow [12]:

$$Rcond_{chip} = \frac{L_{chip}}{k_{chip} \cdot A_{chip}} \tag{1}$$

$$Rcond_{surface} = \frac{L_{surface}}{k_{surface} \cdot A_{surface}} \tag{2}$$

$$Rcond_{pipe} = \frac{\ln\left[\frac{r_2}{r_1}\right]}{2\pi L \cdot k_s} \tag{3}$$

$$Rconv_{pipe} = \frac{1}{\bar{h} \cdot A} \tag{4}$$

$$\bar{h} = \frac{k}{d}\left(0.023 \cdot Re^{0.8} \cdot Pr^{0.4}\right) \tag{5}$$

$$Re = \frac{4\,\dot{m}}{\pi d \mu} \tag{6}$$

$$\frac{T_{mean,outle} - T_{pipe,surface}}{T_{mean,i} - T_{pipe,surface}} = \exp\left[\frac{-\pi d L \bar{h}}{\dot{m} \cdot C_p}\right] \tag{7}$$

$$L_{entrance} = 10d \tag{8}$$

In addition, thermo-physical properties of working fluid (water) are calculated at mean temperature:

$$T_{mean} = \left(T_{mean,outlet} + T_{mean,inlet}\right)/2 \tag{9}$$

The variation of the results obtained from Star CMM+ and EES software is calculated using the relative error percentage equation [13]:

$$T_{j,Error\,\%} = \left[\frac{\left|T_{j,numerical} - T_{j,analytical}\right|}{T_{j,numerical}}\right] \times 100 \tag{10}$$

The Polyhedral mesh structure of the cold plate for the two models using Star CCM+ is shown in Figure 4. The mesh numbers for each components of the cold plate is shown in Table 1. Since the flow is turbulent in the pipe, the selected Reynold number ranged from 400-3600.

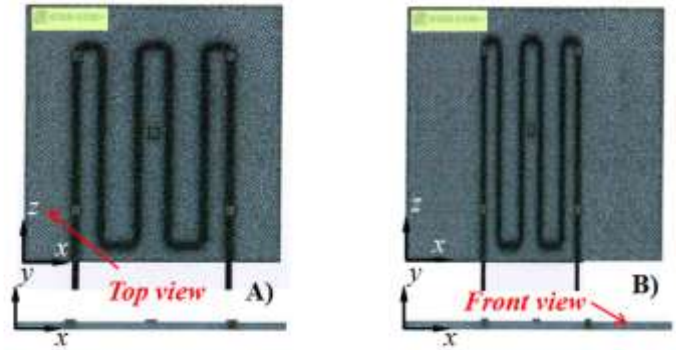

Figure 4. Mesh structure view of the cold plates A) model 1 at S_p=300 mm and B) model 2 at S_p=150 mm.

Table 1. The mesh numbers for each component of the cold plate

Mesh region	Solid	Fluid	Total mesh of cold plate
Cells number	671241	586516	1257757
Faces number	2402412	2158790	4561202
Verts number	1805671	1836548	3642219

3. RESULTS AND DISCUSSION

In this study, the effects of different design parameters of a cold plate on the junction temperature are shown in Figures 5-13. The thermal resistance of each cold plate components in model 1 with and without TIM is shown in Figure 5.

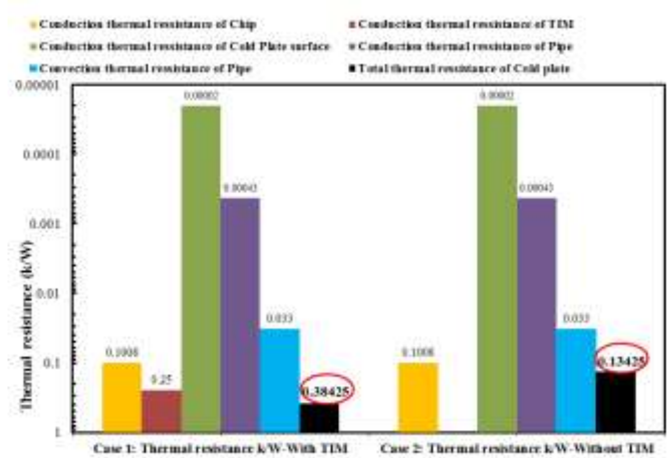

Figure 5. The variation of the thermal resistance of the cold plate components with and without TIM at d_p=12 mm and $\dot{m}$=0.17 kg/s

The results show that the cold plate with TIM has the highest thermal resistance of 0.38 K/W compared to 0.13 K/W for plate without TIM. This is because the thermal interface material has added a thermal resistance of around 0.25 K/W to the overall thermal resistant of the plate. The cold plate pipes has the lowest conduction thermal resistance of all components for both cases.

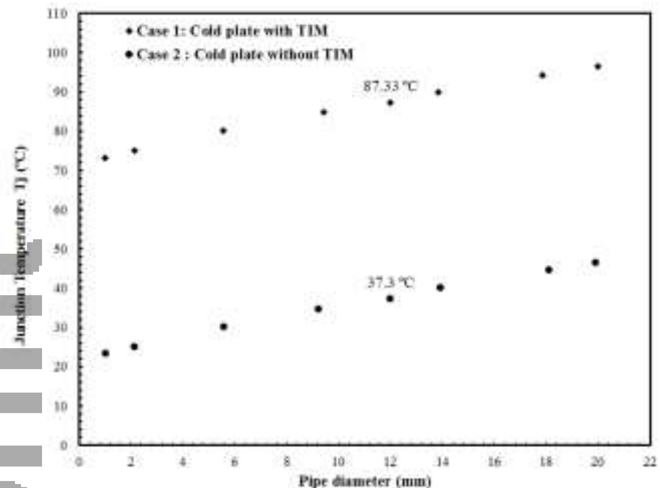

Figure 6. Effect of pipe diameter on the junction temperature with and without TIM at $\dot{m}$=017 kg/s

Figure 6 shows the effect of pipe diameters on the junction temperature at mass flow rate of 0.17 kg/s. The results for both cases shows that the junction temperature raises as the pipe diameters increased. This is due to the reduction in heat transfer rate between the working fluid inside the pipe and external surface of the cold plate.

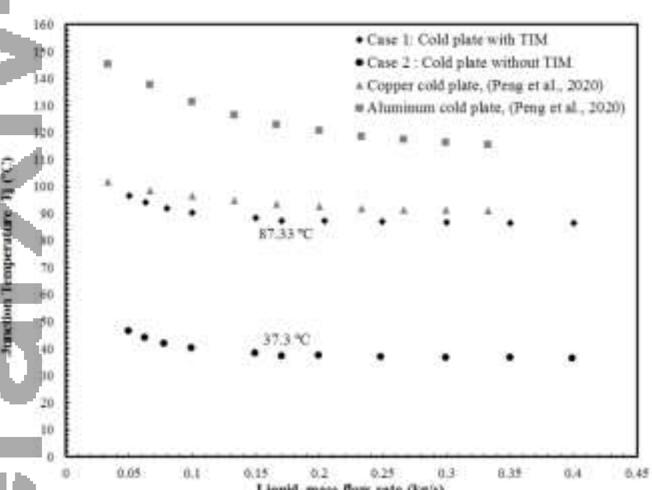

Figure 7. Effect of liquid mass flow rate on the junction temperature with and without TIM at d_p=12 mm

Figure 7 shows the effects of liquid mass flow rate on the junction temperature at a pipe diameter of 12 mm. The results indicate that increasing the water mass flow rate leads to a reduction in the junction temperature. This is because higher mass flow rate means higher heat transfer rate from chips to coolant. These findings are validated by the result obtained from the study conducted by Peng et al., 2020 [14] on a Copper and Aluminum cold plates as shown in Figure 7. Similar behavior was also reported by Siripurapu, K. [15] when comparing two design of cold plate.

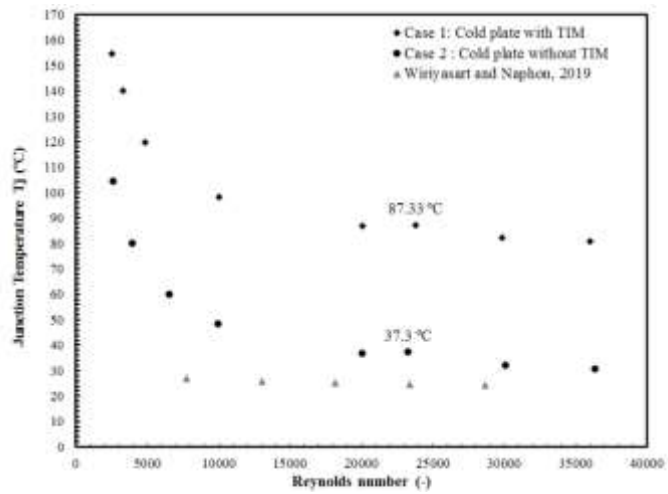

Figure 8. Reynolds number versus the junction temperature with and without TIM at d_p=12 mm and $\dot{m}$=017 kg/s

Figure 8 illustrate the effects of Reynolds number on the junction temperature. The results indicate that the higher Reynolds number, the lower the junction temperature. This is because the more turbulent flow leads to a rise in heat transfer rate with a consequent reduction in junction temperate. Wiriyasart and Naphon, 2019 [16] showed similar behavior of Reynold number with junction temperature which validate our finding as shown in Figure 8.

Figures 6-8 conclude that cold plate without TIM has a lower junction temperature than with a TIM at different design parameters. This is because the thermal resistance for case 2 is lower than case 1 by 65.1 %.

Figure 9 (A and B) shows the temperature distribution on the cold plate in model 1. The results showed that the chip located in the centre of the cold plate has a lower temperature than the other chips for both cases. Hence, this chip location has been selected to measure the junction temperature for both mathematical models to achieve an accurate comparison between them (see Figure 13). The results also reveal that the maximum junction temperature of Case 2 without TIM is lower than Case 1 with TIM by 13.7 % due to the effect of total thermal resistance for the cold plate (see Figure 5).

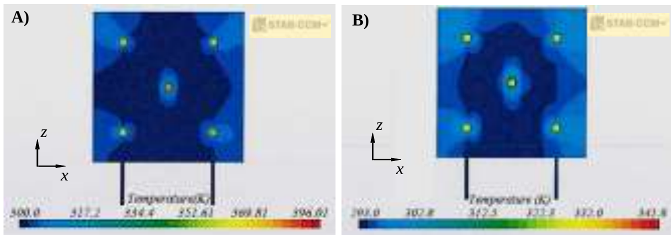

Figure 9. Temperature distribution on the top view of the cold plate model 1 with TIM A) and without TIM B)

Mesh sensitivity analysis has been carried out to determine the optimum mesh cell number MCN. Two different MCN of 1257757 and 913186 have been used to check the accuracy of the numerical results for model 1 without TIM as shown in Figure 10 (A and B). It is clear that increasing the MCN number by 37.3% has no significant effect on the cold plate maximum temperature which showed very little variation of around 0.03%. Hence, MCN of 1257757 has been adopted in the Polyhedral mesh structure 3D simulation (see Table 1).

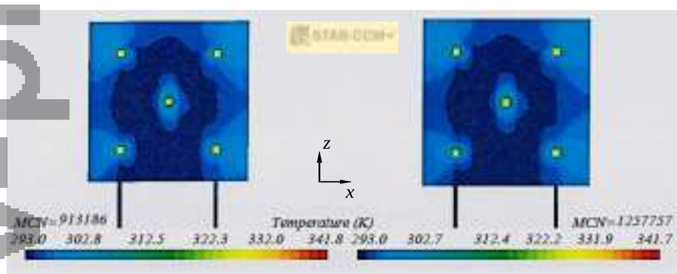

Figure 10. Temperature distribution sensitivity of the cold plate model 1 without TIM to mesh cells number

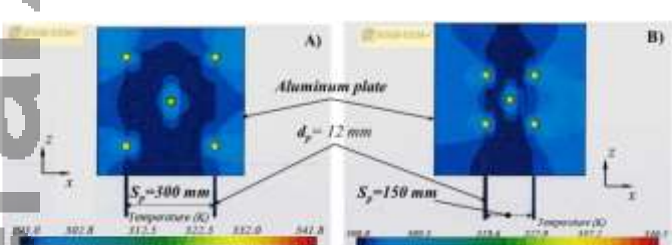

Figure 11. Temperature distribution of the cold plate without TIM A) model 1 and B) model 2

Figure 11 (A and B) shows the temperature distribution of the cold plate for model 1 and 2 without TIM. It is clear that in model 2, the junction temperature is concentrated in a limited area since the chip distance is reduce to 150 mm compared to 300 mm for model 1. The results showed that the highest temperature obtained in model 2 is 346.5 K compared to 341.8 K for model 1 which is due to the lower heat transfer surface area of model 2 cold plate.

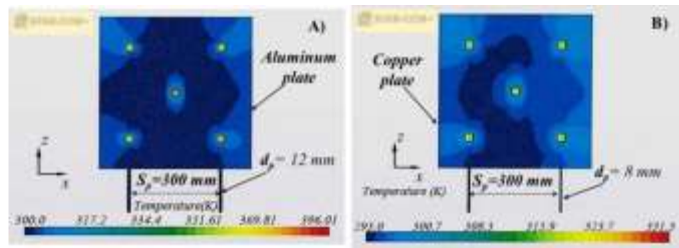

Figure 12. Temperature distribution of the cooling plates with TIM A) model 1 and B) model 3

In model 3, the cold plate material is Copper and the pipe diameter is 8 mm with S_p of 300 mm. Figure 12 (A and B) show the comparison between model 1 and 3 with TIM in term of junction temperature distribution. The result shows that model 3 has lower maximum junction temperature than model 1 by 16.3%. This is because Copper has better thermal conductivity and the turbulent flow inside the cold plate pipes of model 3, which lead to higher heat transfer rate. The current results illustrated the highest temperature in model 3 cold plate is 38.3 °C. These results are comparable to the results obtained by Madani et al. [17] of around 35 °C.

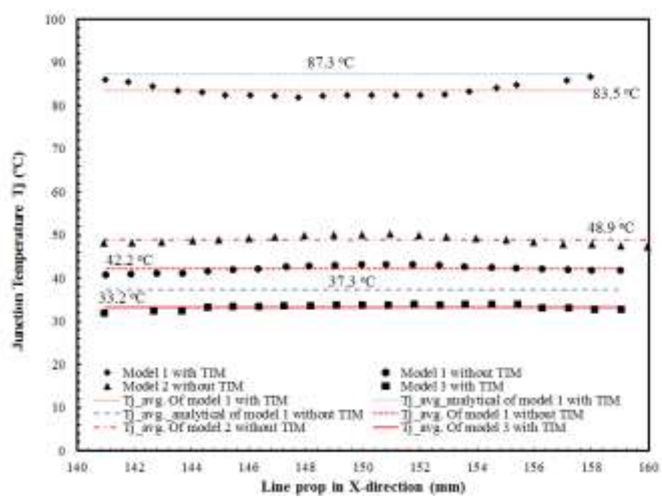

Figure 13. Variation of junction temperature in X-direction for all models of the cold plates with and without TIM

Figure 13 shows the variation in junction temperature along the x-direction in the cold plate with and without TIM for all models. The result shows model 1 with TIM has the highest junction temperature of 83.5 ºC which is due to the effect of total thermal resistant (Figure5). In contrast, model 3 with TIM has achieved 60.2% lower junction temperature than model 1 with TIM. This is because model 3 has 70 % higher thermal conductivity than the other models at 0 ºC.

The results obtained from Star CCM+ and EES for model1 shows good agreement and the error percentages calculated using equation 10 for each case with and without TIM were 4.5 % and 11.5 % respectively.

4. CONCLUSIONS

A Simulation study has been carried out on three proposed models of cold plates to investigate the effect of various design parameters on the junction temperature. Two analysis methods were used, EES program and Star CCM+ for further validation. For cold plate without TIM, model2 showed higher junction temperature of 48.9 ºC compared to 42.2 ºC of model1 due to the more compact design of the chip in model2. Although it is advisable to use the TIM to increase the contact surface area and reduce the thermal resistance between the chip and cold plate. The results showed that using TIM material with cold plate have resulted in higher junction temperature compared to plate without TIM. In terms of the best cold plate design, model3 with TIM has a better heat transfer rate with a consequent reduction in junction temperature from 87.3 ºC to 33.2 ºC.

ACKNOWLEDGEMENT

Authors acknowledges the support of Tikrit University, Diyala University, University of Glasgow, and Ozyegin University.

REFERENCE

[1] W. Nakayama, "Heat in Computers: Applied heat transfer in information technology," *J. Heat Transfer*, vol. 136, no. 1, 2014.

[2] S. G. Kandlikar and C. N. Hayner, "Liquid cooled cold plates for industrial high-power electronic devices thermal design and manufacturing considerations," *Heat Transf. Eng.*, vol. 30, no. 12, pp. 918–930, 2009.

[3] S. Launay, V. Sartre, and J. Bonjour, "Parametric analysis of loop heat pipe operation: a literature review," *Int. J. Therm. Sci.*, vol. 46, no. 7, pp. 621–636, 2007.

[4] J. Choi, Y. H. Kim, Y. Lee, K. J. Lee, and Y. Kim, "Numerical analysis on the performance of cooling plates in a PEFC," *J. Mech. Sci. Technol.*, vol. 22, no. 7, pp. 1417–1425, 2008.

[5] R. Rashad Jassem and T. Khalif Salem, "An Experimental and Numerical Study the Performance of Finned liquid Cold-Plate with Different Operating Conditions," *Int. J. Recent Res. Rev.*, vol. IX, no. 3, pp. 41–46, 2016.

[6] D. Haifeng, S. Ze-chang, W. Xuezhe, and Y. Shu-qiang, "Design and Simulation of Liquid-cooling Plates for Thermal Management of EV Batteries," in *EVS 28 KINTEX , Korea , May 3-6*, 2015.

[7] J. Wang, H. Xu, X. Xu, and C. Pan, "Design and simulation of liquid cooled system for power battery of PHEV," in *IOP Conference Series: Materials Science and Engineering*, 2017, pp. 1–8.

[8] G. Kalaprasad, P. Pradeep, G. Mathew, C. Pavithran, and S. Thomas, "Thermal Conductivity And Thermal Diffusivity Analyses Of Low-Density Polyethylene Composites Reinforced With Sisal, Glass And Intimately Mixed Sisal/Glass Fibers," *Csat*, vol. 60, pp. 2967–2977, 2000.

[9] R. Kuriger and M. Alam, "Thermal Conductivity of Thermoplastic Composites with Submicrometer Carbon fibers," *Exp. Heat Transf.*, vol. 15, no. 1, pp. 19–30, 2002.

[10] H. S. Kim, H. S. Bae, Y. Jaesang, and S. Y. Kim, "Thermal Conductivity of Polymer Composites with the Geometrical Characteristics of Graphene Nano platelets," 2016.

[11] T. Salem, R. Jassem, and S. Farhan, "An experimental and analytical study to show the Effect of the reinforced carbon fiber percentages on the epoxy thermal conductivity and the heatsink performance," *Int. J. Sci. Eng. Appl. Sci.*, vol. 2, no. 8, pp. 96–110, 2016.

[12] J. P. Holman, *Heat Transfer*, 10th ed. McGraw-Hill Series in Mechanical Engineering, Avenue of the Americas, New York, NY 10020., 2010.

[13] N. Ahmadi, A. Dadvand, I. Mirzaei, and S. Rezazadeh, "Modeling of polymer electrolyte membrane fuel cell with circular and elliptical cross-section gas channels: A novel procedure," *Int. J. Energy Res.*, vol. 42, no. 8, pp. 2805–2822, 2018.

[14] L. Peng *et al.*, "Method for obtaining junction temperature of power semiconductor devices combining computational fluid dynamics and thermal network," *Nucl. Instruments Methods Phys. Res. Sect. A Accel. Spectrometers, Detect. Assoc. Equip.*, vol. 976, no. 164260, pp. 1–10, 2020.

[15] K. C. Siripurapu, "Thermal Management Of High Power Multi Chip Module by Design Optimization of Segregated Serpentine Flow Cold Plate," TEXAS, 2017.

[16] S. Wiriyasart and P. Naphon, "Liquid impingement cooling of cold plate heat sink with different fin configurations: High heat flux applications," *Int. J. Heat Mass Transf.*, vol. 140, pp. 281–292, 2019.

[17] S. S. Madani, E. Schaltz, and S. K. Kær, "Thermal analysis of cold plate with different configurations for thermal management of a lithium-ion battery," *Batteries*, vol. 6, no. 17, pp. 1–11, 2020.

